33rd Annual International Conference of the IEEE EMBS
Boston, Massachusetts USA, August 30 - September 3, 2011

Geometric modeling of pelvic organs

Thierry Bay, Jean-Christophe Chambelland, Romain Raffin, Marc Daniel and Marc-Emmanuel Bellemare

***Abstract*— The pelvic floor can be subjected to different disorders, coming from a physiological change in the spatial configuration of the organs of interest: the bladder, the rectum, the uterus and the vagina. However, resort to surgery to replace them is complicated to achieve. In order to support the decision of the surgeon as to the invasive method to use for the patient, the MoDyPe (Pelvis Dynamics Modeling) project was launched, aiming at building a patient specific pelvic organ behavior.**

Our approach consists in creating thick surfaces of hollow organs, using periodic B-splines and offsets, then in controlling their discretization and in exporting a hexahedral model to provide input data for the study on the dynamics of the soft bodies of interest.

From a segmentation step providing a dataset of 3D points, a function is built to measure the bidirectional distance between the surface and the data. It is minimized with an alternate iterative Hoschek-like method, by updating the parametric map and moving the control points. Several offsets of the base surface are then created to build up the thickness of the organ.

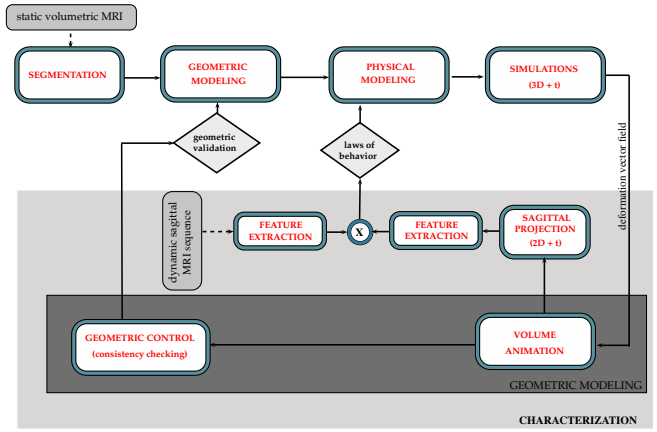

Fig. 1. Steps of MoDyPe process

I. INTRODUCTION

Information Technology modeling of organs remains a difficult problem. This is due to the several factors that need to be accounted for during the modeling like hollow organs, soft tissues, and complex *in vivo* behaviors. This modeling is important in several processes, such as simulating the movement of organs or surgical planning.

The field of interest on which we have focused refers to the pelvic floor and the following organs: the bladder, the rectum, the uterus and the vagina. As a matter of fact, due to changes in their spatial configuration, disorders can come forth, like prolapse, cystocele and rectocele. Although surgery can restore the balance of their initial layout, MoDyPe project intends to develop a specific-patient decision support software in order to evaluate the surgical gesture and the invasive procedures to be used.

Some approaches have already been developed. However, either the method underestimates the importance of geometric modeling by merging this field with physical modeling [1], or the algorithm lacks accuracy due to an unconstrained tetrahedrization of the model [2]. This latter puts forward a mass-spring system to simulate the organs behavior under stress. Although it leads to rapid results, the generation of degenerate elements is inevitable, which affects the accuracy of calculations. Other projects have investigated the anatomical objects [3], but none of them has considered the organs as hollow and thick-surfaced volume.

The approach proposed in this paper is implied into a feedback loop, in between a segmentation step acquiring data sets and a physical modeling step to simulate the organs behaviors (calculations with finite elements).

B-splines [4] are used to reproduce more closely the organs features (hollow and closed shape without sharp edges). The continuous representation gives advantages: ease to move on the surfaces, smooth and controllable shapes.

Our inputs come from physical measurements from static MRI (ITK-SNAP, *www.itksnap.org*). But even though experts supervise data acquisition, human action can induce a lack of accuracy. Further to the potential presence of parasites, an approximate approach is considered for stability of the model. The construction of an organ consists of three main stages: surface reconstruction of the outer layer from the data, addition of a thickness on the organs by offsets and hexaedrization of the hollow volumes to provide a mesh to the input of the physical modeling process.

The global process of MoDyPe project is presented in a first part. Then, the surface reconstruction is put forward, followed by the offset formulation. For both sections, results are discussed to show consistency of the developed methods.

II. A FEEDBACK-LOOP PROCESS

Our method is integrated in a process divided into four modules. Each module interoperates with the others through specific interfaces (Fig. 1).

From a static MRI of the patient, the first module takes care of the segmentation that generates a set of 3D points. They belong to the surface of the organs of interest. This step

T. Bay (thierry.bay@lsis.org), J-C. Chambelland (chambelland@univmed.fr), R. Raffin (romain.raffin@lsis.org) and M. Daniel (marc.daniel@lsis.org) are from the G-MOD group of LSIS Laboratory (U.M.R. C.N.R.S. 6168). ESIL, Campus de Luminy, Case postale 925, 13288 Marseille Cedex 9 - France. Tel: 33491828525, Fax: +33491828511.

M-E. Bellemare (marc-emmanuel.bellemare@lsis.org) is with the I&M group of LSIS Laboratory. Domaine universitaire de St Jérôme 13397 Marseille Cedex 20 France. Tel: 33491056024, Fax: +33491056033.

interacts directly with the geometric modeling by providing the input data. The second module reconstructs the surfaces of the outer membranes, and builds the thickness for each organ (thanks to medical knowledge). A closed, hollow, and thick-surfaced volume is then created and discretized in order to provide a hexahedral mesh. The third module is physical modeling. The mesh is retrieved and sought to replicate the movements of organs under stress by determining the underlying laws of behavior through simulations. A sequence of images is produced by projecting the outputs of the simulations in a sagittal plane. The characterization step realignes and characterizes the simulated movements of organs and compares the results with a ground-truth (dynamic MRI).

The feedback loop takes action if the characterization step is not satisfied according to the consistency of results. Two possible returns are available. A control of geometric modeling is added after the simulations to assess the geometric consistency of hexahedral elements, and thus to detect the possible presence of degenerate elements (the study of variation in the shape of hexahedron). Local operations of decimation and refinement are then applied, to improve the accuracy of the calculations and avoid erroneous results. The second return is linked to the law of behavior which is modified in case of inconclusive results, in terms of non realistic movements.

This loop is repeated until the accuracy (criteria set by the characterization step) is reached. It divides the process into three distinct roles: segmentation and geometric modeling are used to support the model, the physical modeling creates a dynamic mesh of organs, and the realignment of the characterization step monitors the results compliancy.

However, each module works independantly yet. Therefore only geometric modeling work are put forward afterward.

III. SURFACE RECONSTRUCTION

In order to keep the advantages of the parametric approach [5]–[7], a B-spline formulation is used to reconstruct the surface of the organs. The chosen optimization method is an alternate iterative technique [8], [9], providing a compromise between complexity and accuracy. The base surface is a k-order periodic B-spline generated from a semi-toroidal surface to have C^{k-2} continuity and therefore a "smooth" shape for the closed surface.

Periodicity of a B-spline ensures tangent and curvature continuity across the entire parametric domain. For a k-order curve, the $k-1$ first control points and parametric intervals must be superimposed on the $k-1$ last ones. This principle is applicable to surfaces (surfaces also known as tori). This property is taken into account in the surface formulation by an alteration of the nodal vectors and the control network [3]. However, working on half the form only gives the same results with less data (Fig. 2).

The f function characterizes the distance between the parametric surface S and the data points $\{D_s\}_{s=0}^{N}$. Let $\{P_{i,j}\}$ be the $(n+1)\times(m+1)$ control points of S in $\mathbb{R}^3$ and let E be the sampling of S ($card(E)=M$) with a *fixed* uniform parametric map. Let U and V be the vectors containing

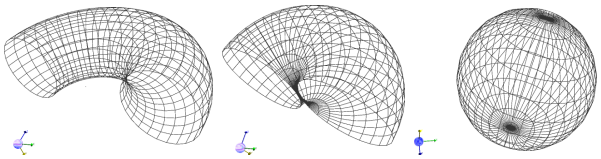

(a) Half-torus from a 1-genus torus (b) Collar reduction (c) Degenerate torus without collar

Fig. 2. Half-tori build with biperiodicity

the values of the parameterization (eg. the parametric pair $(u_.,v_.)_k$ will be associated to the k^{th} sampling point).

The error function (1) is separated into two sub-functions (sums of squares of distances) illustrated by Fig. 3. The first sub-function $f_{D\to E}$, defined by (2), puts forward dissimilarity of D over the sampling E, and the second $f_{E\to D}$ characterizes dissimilarity of E over D:

$$f = f_{D\to E}(P,U,V) + f_{E\to D}(P,U,V) \qquad (1)$$

The sub-function $f_{D\to E}$ associates each point of D with its 0-order projection on S (the closest sampled point to the datum). It is defined by :

$$f_{D\to E}(P,U,V) = \sum_{s=0}^{N} \|D_s - S((u_.,v_.)_\star)\|^2, \qquad (2)$$

with: $\|D_s - S((u_.,v_.)_\star)\|^2 = \min_j \|D_s - S((u_.,v_.)_j)\|^2$.

In the same principle, the second sub-function $f_{E\to D}$ associates each sampled point to the closest datum.

The iterative minimization is based on the alternation of two steps for each sub-function. The first step constructs f and consists in updating the graph of connections (0-order projections) between the sets D and E. A gradient descent with optimal step method is then applied to reduce f. Let f_c and f_{c+1} be the f values at iterations c and $c+1$. The descent step a_c at the c^{th} iteration is calculated such that $f_{c+1}(P - a_c\nabla^P f_c, U, V)$ is minimal.

A. Assets and drawbacks

This formulation of f intends to avoid minimization problems for complex forms (e.g. variations of curvature, excavations). This produces a "smooth" shape without sharp edges. Furthermore, working on one half of the torus prevents unnecessary overlapping control points that would occur with a full one (creating a stack of surfaces). After fitting, the

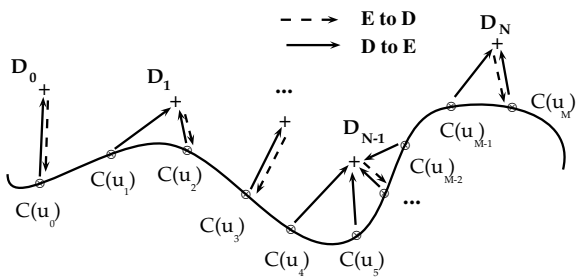

Fig. 3. Distances for the two sub-functions with a curve C

discretization of S is in a good configuration to work on the thickness of the organs (Section IV).

However, the initialization of the base surface is located at the center of the cloud of points. The initial surface does not facilitate the fitting process. Besides, the graph of connections is defined globally. Computation times are mainly related to the heuristic used in the first step for the matching between the sampling and the data.

B. Results and discussions

The simulations were performed with an Intel Core i7 M620 (2.67 GHz, 4 GB RAM). The surface reconstruction explained in section III is applied to the four organs. The numerical results below are concerning the bladder. Its data file include 45000 points and its oriented bounding box is $107 \times 69 \times 74$ mm. The initial parametric surface is a 4-order B-spline in both directions and has a sampling cardinality similar to the dataset cardinality.

Table I references computation time (min) needed for smoothing the surface of a bladder and the Mean Square Error (mm). The MSE has an initial value of 13.75. Several dimensions of the control network are compared. The process was stopped after 5, 10 and 15 iterations.

The results in Table I put forward the decrease of the MSE during iterations. The increase of the computation time is related to the larger control network. However, it is considered in the steepest descent step. Most of the calculations is used for the cost-consuming distances evaluation step. We plan to explore parallel implementation of our algorithm. This will dramatically pull down the duration, as distance computations of couple of points are not self-dependent. A *Quadtree* approach to obtain the neighborhood data points should reduce the computation times as well. Furthermore, we can put forward that we get MSE values smaller than the 1 mm acquisition accuracy coming from MRI resolution. Finally, the method is sensitive to the initial location of the surface, like any iterative method (risk of network overlays when the control points are moved when the initialization is too far from the form to achieve). The use of PCA to describe the direction of the maximum variance will facilitate the initial positioning of control points.

The bladder surface computation results are similar to those obtained with the other organs.

Fig. 4(a), 4(b) and 4(c) illustrate the four pelvic organs after 15 iterations. Once this reconstruction step is achieved, we use this surface to define thick organs by offsetting.

TABLE I

SURFACE RECONSTRUCTION PROCESS OF A BLADDER, WITH THE COMPUTATION TIME (MIN) AND THE MSE (MM)

	Control network dimensions					
	11×19		13×23		15×27	
	time	MSE	time	MSE	time	MSE
5 iterations	10.35	2.57	9.7	1.61	11.79	1.05
10 iterations	19.87	1.02	20.1	0.84	23.9	0.76
15 iterations	29.77	0.88	30.57	0.73	33.6	0.67

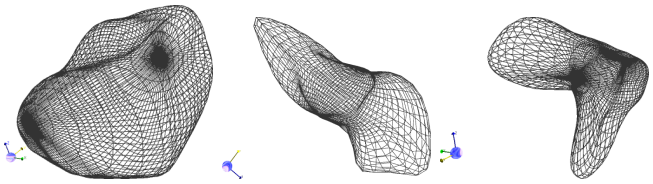

(a) Bladder (b) Rectum (c) Uterus/vagina

Fig. 4. Reconstruction for 15 iterations with 13×23 control network and a sampling cardinality similar to the dataset cardinality

IV. THICK SURFACES BY OFFSETS

The surface reconstruction process employed in Section III enables us to work on the thickness of the organs thanks to the offset formulation, as in [10] and [11]. This thickness is controlled by four distincts parameters: an offset-direction governed by the oriented normal to the surface (towards the inside or the outside of the organ), an offset-distance d (real thickness of the organ membrane), the number of layers N_{lay} in the thickness and a coefficient a for the layer distribution.

The offset S_o of a surface S at a distance d of S, as in (3), is constructed in three stages. The first one consists in discretizing S. Then, the normal vectors at the discrete points of S are calculated. Finally, an interpolation of the offset-cloud creates a parametric offset-surface S_o, as:

$$S_o(u,v) = S(u,v) + d\frac{\frac{\partial S}{\partial u} \times \frac{\partial S}{\partial v}}{\left\| \frac{\partial S}{\partial u} \times \frac{\partial S}{\partial v} \right\|} \tag{3}$$

The creation of a single offset-surface would not be enough to achieve sufficient accuracy in the calculations. Let $\{h_i\}_{i=1}^{N_{lay}}$ be all the thicknesses considered. Each value corresponds to a distance from the base surface S. The establishment of a "distancer" gives a geometric progression of these distances, considering a smaller thickness at the ends of the membrane (the outermost and the innermost layers) where the deformations are more important. A distribution control is possible with the parameter a. The more a tends to 0, the more the surface layers will be located next to the innermost and the outermost layers. *A contrario*, if a tends to 1 the layers will go towards the average layer.

In the case where N_{lay} is odd, we have:

$$\begin{cases} h_i = \frac{1}{2}\frac{\sum_{j=1}^{i} a^j}{\sum_{k=1}^{\frac{N_{lay}-1}{2}} a^k} d \\ h_{N_{lay}-i-1} = d - h_i \end{cases} \quad \forall i = \left\{0, \cdots, \frac{N_{lay}-1}{2}\right\} \tag{4}$$

The same principle is used for an even number of layers (paying attention near the center of the thick membrane).

A change of scale replaces a within the interval $[0,1]$ for convenience. With the distancer, a set of surfaces $\{S_i\}_{i=2}^{N_{lay}}$ is created, with $S_1 = S$. We have, $\forall i \in \{1, \ldots, N_{lay}-1\}$:

$$S_{i+1}(u,v) = S_i(u,v) + h_i\frac{\frac{\partial S_i}{\partial u} \times \frac{\partial S_i}{\partial v}}{\left\| \frac{\partial S_i}{\partial u} \times \frac{\partial S_i}{\partial v} \right\|} \tag{5}$$

For a fixed thickness, a uniform discretization is applied. However, we have to ensure an immediate correspondence between the hexahedral elements from a layer to another.

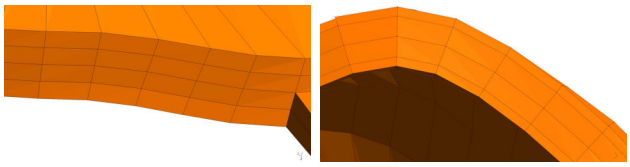

(a) Uniform distribution: $a = 0.5$ (b) Towards extremities: $a = 0.3$

Fig. 5. Influence of the parameter a (GMSH viewer, *geuz.org/gmsh*)

A. Assets and drawbacks

The offset construction process can get more realistic organs by considering their non-negligible thickness. But the problem of offset methods is due to self-intersections [10]. Overlappings of the surface are created when the absolute value of the offset distance exceeds the minimum radius of curvature in the concave regions. From the shape of our organs, global self-intersections are not met. But since we get the offsets from an interpolation, the sampling features like the curvatures are not taken into account during the fitting process to prevent local cranklings.

B. Results and discussions

Due to the bladder dimensions, the chosen thickness is 5 mm [12]. The offset-direction is towards the inside, since the external hull is built. The influence of the stretching parameter a is illustrated by Fig. 5(a) and 5(b). With $a = 0.5$, we get the same thickness for each layer; with $a = 0.3$, the layers are pushed towards the inner and the outer boundaries of the membrane.

However, the values of the other parameters a and N_{lay} are not adjustable according to a heuristic method for the moment. The value of N_{lay} could be related to the ouput constraint requiring regular mesh elements. Therefore a sampling-based heuristic could be applied in 3D to provide nearly cubic elements. Concerning the coefficient a, a sensitivity analysis could be performed to quantify its influence on the results. We could check if the calculations by finite elements would be more accurate with thinner surfaces located next to a border with a different density area.

The presence of local cranklings is observed (Fig. 6). It produces degenerate elements that will provide erroneous results. An idea would be to apply the surface reconstruction process on the offset-sampling, that would guarantee a C^{k-2} continuity to the offset.

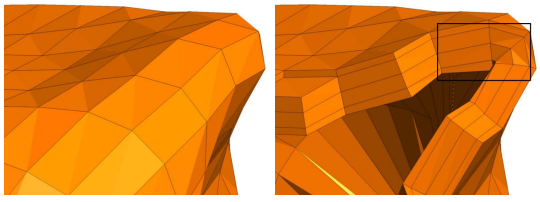

(a) Rough region of a bladder (b) Internal self-intersection

Fig. 6. A rough discretization of a bladder: (a) outer layer, (b) self-intersections to be corrected (GMSH viewer)

V. CONCLUSIONS AND FUTURE WORKS

We have presented a process to construct organs of the pelvic region with a thick surface. The periodic base surface is created from a degenerate half-torus, avoiding the problems of singularities obtained with uniform nodal vectors. The non-negligible thickness of the organs is taken into account to improve the realism of the reconstructions, and will highlight the density difference between the inside and the outside of the organs.

The addition of a dynamic insertion of control points in the iterative minimization process should lead to a better decreased MSE. Besides, the validation of the updated parametric map (Section III) requires a comparison with a projection method as in [9]. Even though the distances evaluation step is cost-consuming, different solutions could be performed to decrease the duration thanks to algorithmic methods, like PCA or *Quadtree*. Regarding offsets, the local self-intersections must be managed. But a solution would be to apply our surface reconstruction process on the offset-samplings. A heuristic to determine the parameters values N_{lay} and a has to be defined and applied yet.

The use of this geometric model for the optimization of FEM calculations for the simulations and the characterization module is a work in progress.

VI. ACKNOWLEDGMENTS

This work is supported by the French National Research Agency (ANR) under reference ANR-09-SYSC-008.

REFERENCES

[1] M. Boubaker, M. Haboussi, J.-F. Ganghoffer, and P. Aletti, "Finite element simulation of interactions between pelvic organs: Predictive model of the prostate motion in the context of radiotherapy," *Journal of Biomechanics*, vol. 42, no. 12, pp. 1862–1868, 2009.

[2] M.-E. Bellemare, N. Pirro, L. Marsac, and O. Durieux, "Toward the Simulation of the Strain of Female Pelvic Organs," in *EMBC07, 29th IEEE EMBS Annual International Conference*, Aug. 2007, pp. 2756–2759.

[3] F. Jaillet, B. Shariat, and D. Vorpe, "Periodic b-spline surface skinning of anatomic shapes," in *9th Canadian Conference on Computational Geometry*, Aug. 1997, pp. 119–210.

[4] L. Piegl and W. Tiller, *The NURBS book (2nd ed.)*. Springer-Verlag New York, Inc., 1997.

[5] I. D. Faux and M. J. Pratt, *Computational Geometry for Design and Manufacture*. New York, NY, USA: Halsted Press, 1979.

[6] G. Farin, *Curves and surfaces for computer aided geometric design: a practical guide*. San Diego, CA, USA: Academic Press Professional, Inc., 1988.

[7] J. Hoschek and D. Lasser, *Fundamentals of computer aided geometric design*. Natick, MA, USA: A. K. Peters, Ltd., 1993, translator-Schumaker, Larry L.

[8] J. Hoschek, "Intrinsic parametrization for approximation," *Computer Aided Geometric Design*, vol. 5, no. 1, pp. 27–31, 1988.

[9] J. Chambelland and M. Daniel, "An iterative method for rational pole curve fitting," in *WSCG 2006 conference proceedings*, Feb. 2006, pp. 39–46.

[10] T. Maekawa, "An overview of offset curves and surfaces," *Computer-Aided Design*, vol. 31, no. 3, pp. 165–173, 1999.

[11] M. A. Kulczycka and L. J. Nachman, "Qualitative and quantitative comparisons of B-spline offset surface approximation methods," *Computer-Aided Design*, vol. 34, no. 1, pp. 19–26, 2002.

[12] M. Schuenke, E. Schulte, U. Schumacher, L. Ross, E. Lamperti, M. Voll, and K. Wesker, *Neck and Internal Organs (THIEME Atlas of Anatomy)*. Thieme, Mar. 2010, vol. 20, ch. 2, p. 237.